Immersion precipitation route towards high performance thick and flexible electrodes for Li-ion batteries

Harks, Peter Paul R.M.L.; Robledo, Carla B.; George, Chandramohan; Wang, Chao; van Dijk, Thomas; Sturkenboom, Leon; Roesink, Erik D.W.; Mulder, Fokko M.

DOI
10.1016/j.jpowsour.2019.227200

Publication date
2019

Document Version
Final published version

Published in
Journal of Power Sources

Citation (APA)
Harks, P. P. R. M. L., Robledo, C. B., George, C., Wang, C., van Dijk, T., Sturkenboom, L., Roesink, E. D. W., & Mulder, F. M. (2019). Immersion precipitation route towards high performance thick and flexible electrodes for Li-ion batteries. *Journal of Power Sources*, *441*, Article 227200. https://doi.org/10.1016/j.jpowsour.2019.227200

Journal of Power Sources 441 (2019) 227200

Contents lists available at ScienceDirect

Journal of Power Sources

journal homepage: www.elsevier.com/locate/jpowsour

Immersion precipitation route towards high performance thick and flexible electrodes for Li-ion batteries

Peter-Paul R.M.L. Harks [a], Carla B. Robledo [a,b], Chandramohan George [c], Chao Wang [c], Thomas van Dijk [d], Leon Sturkenboom [d], Erik D.W. Roesink [e], Fokko M. Mulder [a,*]

[a] Materials for Energy Conversion and Storage (MECS), Department of Chemical Engineering, Delft University of Technology, P.O. Box 5045, 2600 GA, Delft, the Netherlands
[b] Energy Technology, Department Process and Energy, Delft University of Technology, Leeghwaterstraat 39, 2628 CB, Delft, the Netherlands
[c] Department of Radiation Science and Technology, Delft University of Technology, Mekelweg 15, 2629JB, Delft, the Netherlands
[d] E-Stone, Westervoortsedijk 71 – S, 6827 AV, Arnhem, the Netherlands
[e] Membrane Science and Technology, MESA+ Institute for Nanotechnology, University of Twente, P.O. Box 217, 7500 AE, Enschede, the Netherlands

HIGHLIGHTS

- Immersion precipitation offers a new route to fabricate battery electrodes.
- The electrodes can be substrate-based or self-supporting and are highly flexible.
- Environmentally friendly solvents can be used.

ARTICLE INFO

Keywords:
Phase inversion
Immersion precipitation
Batteries
Electrodes
Flexible batteries

ABSTRACT

Enabling the transition to renewable power sources requires further optimization of batteries in terms of energy/power density and cost-effectiveness. Increasing the practical thickness of Li ion battery electrodes not only can improve energy density on cell level but reduces manufacturing cost. However, thick electrodes exhibit sluggish charge-transport kinetics and are mechanically less stable, typically resulting in substandard battery performance compared to the current commercial standards (~50 μm). Here we disclose a novel method based on immersion precipitation by employing a non-solvent to solidify the battery binder, instead of solvent evaporation. This method allows for the fabrication of thick and suitable density electrodes (>100 μm with ultra-high mass loading) offering excellent electrochemical performance and mechanical stability. Using commercial electrode active materials at a remarkable mass-loading of 24 mg cm^{-2}, the electrodes processed via immersion method are shown to deliver 3.5 mAh cm^{-2} at a rate of 2C and operate at rates up to 10C. As additional figure of merit, this method produces electrodes that are both stand-alone and highly flexible, which have been evaluated in flexible full-cells. Furthermore, via immersion precipitation the commonly used more toxic N-Methyl-2-pyrrolidone can be supplanted by environmentally benign dimethyl sulfoxide as solvent for processing electrode layers.

1. Introduction

Li-ion batteries (LIB) with high energy density and adequate power output are required to enable heavy-duty applications such as power tools, drones/robots, power storage from intermittent energy sources [1], and electric vehicles with optimal driving range. To put these in practice a rapid improvement in both battery energy/power density and cost-effectiveness is needed. A straightforward way to improve the energy density of batteries is to adopt thicker electrodes. This increases the energy density on the cell level and reduces the cost as it minimizes inactive components such as current collectors and separators, and requires only fewer layers to be processed (see Fig. 1a and b) [2,3]. If one assumes doubling the electrode thickness from 50 to 100 μm, the increase in volumetric and gravimetric energy density (without considering the packaging) can be estimated to be ~16 and 20%, respectively (see Supporting Information). The cost reduction as a result of doubling the electrode thickness has been calculated to be in the range of 16–25% [2,3]. However, there are two formidable hurdles en route to achieving

* Corresponding author.
E-mail address: f.m.mulder@tudelft.nl (F.M. Mulder).

https://doi.org/10.1016/j.jpowsour.2019.227200
Received 13 June 2019; Received in revised form 5 September 2019; Accepted 22 September 2019
Available online 17 October 2019

operable thick battery electrodes. Firstly, the commercial LIB-electrodes are produced by coating a slurry that is prepared by mixing a liquid solvent, a polymeric binder, active material and conductive carbon on metal foils as current collector (Cu or Al). The slot-die coated metal foils are then dried and followed by roll-mill pressing. For research purposes the method remains mostly unaltered, however often a doctor blade technique is used for casting [4]. Unfortunately, thick coatings are prone to form cracks due to high stress developed during drying, and tend to crumble away or detach from metal current collectors and mechanically weak electrodes are extremely difficult to process using roll-to-roll coaters. Consequently, these issues limit electrode thickness for this method to the maximum of 100 μm, where high-performance LIB electrodes in practice even have thinner electrodes of 50–60 μm [3,5,6]. In addition, the current process does not impart electrodes with sufficient mechanical strength and resilience for applications such as wearable electronics, bendable smart phones and medical implants. To date, the development of flexible electrodes relies heavily on the use of expensive and advanced carbon structures such as carbon nanotubes, nanofibers and graphene (oxide) to accommodate flexibility [7,8].

Secondly, the diffusion limited ionic resistance increases exponentially with increasing thickness, leading to poor electrochemical performance and drastic reduction in both energy/power capabilities. In fact the extent to which electrodes can be thickened depends on whether battery performance still meets the power/energy requirements of the given application (e.g. portable electronics or electric vehicles). Therefore, unless considerable improvements on thick electrodes in terms of charge transport kinetics and mechanical integrity are achieved, it is highly unlikely to increase the energy density by increasing the thickness, without compromising the power density. This severely bottlenecks the fabrication of thick electrodes on commercial scale to date.

Surprisingly, research on the fabrication and optimization of thick electrodes is limited [9–17], let alone those that are capable of being self-supporting or flexible. Furthermore, much of battery materials research is conducted on thin and low mass-loading electrodes (~1 mg cm^{-2}), which cannot be directly used to extrapolate and predict the performance of thick electrodes that are plagued by severe mechanical and charge transport issues [18–20]. It is therefore difficult to translate results based on low mass loadings into real-world batteries. Also, it is often not indicated whether such special methods and/or conductive additives adopted in research can actually make the fabrication of battery electrodes to be economically feasible and/or scalable.

In this work we present a versatile method for the fabrication of high performance thick and flexible electrodes by a phase inversion process, namely immersion precipitation. This process allows for the choice between substrate based (with current collectors) and self-supporting electrodes (stand-alone). To show the versatility of the method and its relevance to commercial battery electrodes, we tested electrodes produced by this method using commercial lithium titanate ($Li_4Ti_5O_{12}$, or LTO), lithium iron phosphate (LFP) and lithium cobalt oxide (LCO) as active materials. The obtained thick electrodes are flexible, mechanically stable, and can easily be made thicker than current standards. Electrodes with a high mass-loading of 24 mg cm^{-2}, corresponding to a capacity of 4 mAh cm^{-2}, can be cycled at high C-rates.

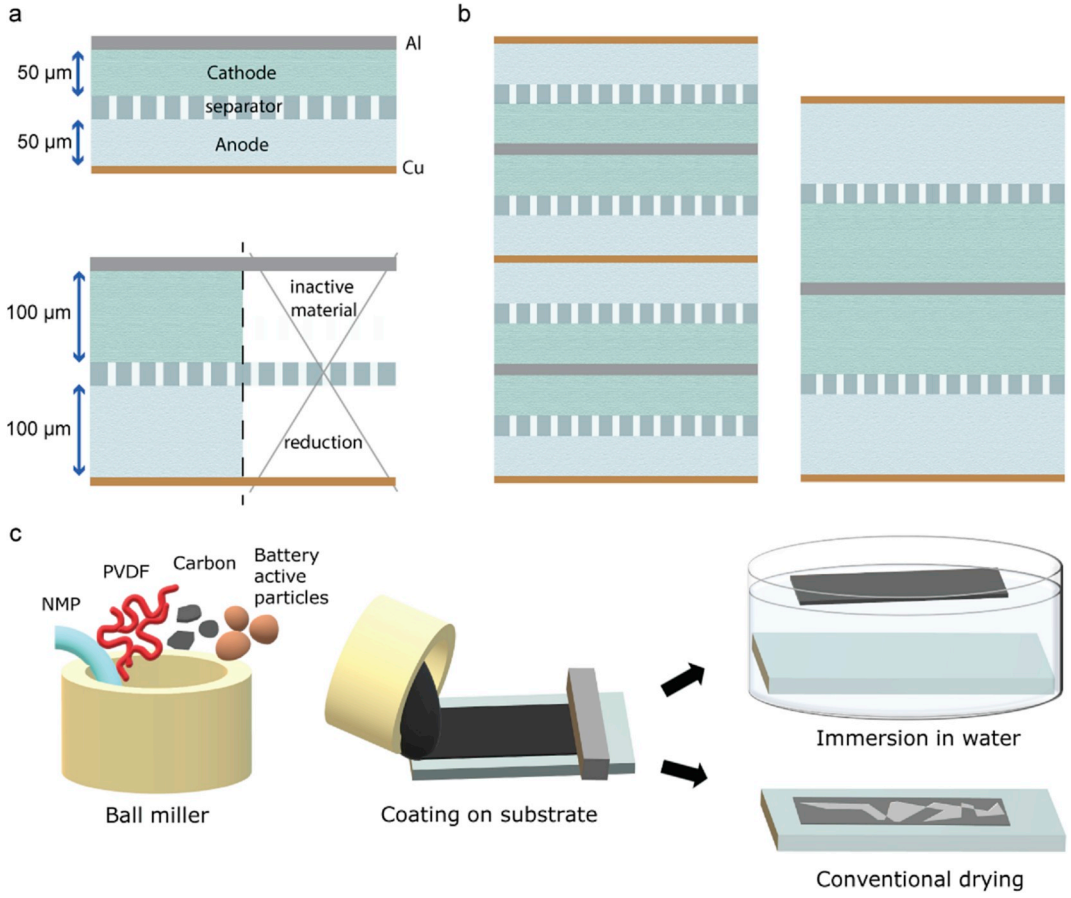

Fig. 1. Schematic representation of doubling battery electrode thickness. a) A conventional battery based on thin electrodes and a battery with the same theoretical capacity, but based on twice as thick electrodes, resulting in a reduction of inactive materials, and thus costs. b) The battery with two times thicker electrodes at the right has the same amount of active material in a smaller volume and with lower mass because of the lower number of current collectors and separators, needing a lower amount of layers to process. The components are drawn to scale; separator 25 μm, Cu 9 μm, Al 15 μm. c) The fabrication of self-supporting electrodes using immersion precipitation.

2. Methods

2.1. Electrode fabrication by immersion precipitation

First, polyvinylidene fluoride (PVDF) (Sigma Aldrich) and either N-methyl-2-pyrrolidone (NMP) (Sigma Aldrich) or dimethyl sulfoxide (DMSO) (sigma Aldrich), were mixed in a planetary ball mill. The mass ratio of PVDF:solvent ranged from 1:10 to 1:20. Then, commercial LTO (particle size ~150 nm, Süd-Chemie) or LFP (carbon coated particles 140 nm, Phostech) or LCO (Sigma Aldrich) powder and carbon black Super P (Timcal) were added and mixed, to obtain a viscous, paste-like, slurry. Subsequently, the slurry was casted on aluminum foil or a glass plate by a doctor blade technique and immersed in a water bath. The Al-foil based electrodes were immersed for 5 s. The short period of time in contact with water is sufficient to induce the phase inversion but does not cause delamination. The electrodes casted on glass were immersed for a longer period of time (approximately 1 min) after which they spontaneously released, yielding a flexible self-supporting membrane. Fig. 1c shows a schematic representation of this procedure. The electrodes were not compressed, unless otherwise stated. The electrochemical measurements in this work were performed on self-supporting electrodes with a mass ratio of 90:5:5, active materials, Super P, PVDF, respectively. The (apparent) porosity was calculated based on the geometry and weight of the electrodes and the density of the constituents, and ranged from 60 to 67% for non-calendared electrodes.

2.2. Electrode characterization

The morphology of the electrodes was examined with a JEOL JSM-IT100 scanning electron microscope, operating at an acceleration voltage of 5 kV.

Impedance spectroscopy was executed with an Autolab PGSTAT302 N, for frequencies ranging from 10^6 to 0.1 Hz, with an AC signal of 10 mV. The DC resistance was obtained through Ohms law, by placing the electrodes between two metal connectors and measuring the current when applying 0.1V.

Tensile strength measurements were performed with a TA Instruments DMA Q800, with a displacement of 100 μm/min.

The porosity was investigated by mercury intrusion porosimetry with a Micrometrics PoroSizer 9320 applying a maximum intrusion pressure of 207 MPa. In addition to the pore volume and pore size distribution, the permeability was obtained by using an empirical correlation established by Katz et al. [21,22] which relates permeability to a critical pore diameter. The critical pore diameter is obtained by identifying the first inflection point on the steeply rising range of the intrusion curve. This point corresponds closely to the pore size at which mercury first finds a path spanning the sample. The samples were coarse powders, scraped off the aluminum current collector or fragmented self-supporting films. The measured inter particle volume (pore sizes > 100 μm) was discarded and not shown.

2.3. Electrochemical measurements

Prior to measurements, the electrodes were dried at 80 °C in a vacuum oven overnight. The employed electrochemical cells were purpose-built prototypes consisting of two stainless steel vacuum flanges, described elsewhere [23]. The cells were assembled inside an Ar filled glovebox with oxygen and water content less than 1 ppm. Lithium foil was used as the counter and reference electrode, combined with a glass fiber (Whatman) separator and the working electrodes to make up the cell. As electrolyte a solution of 1 M $LiPF_6$ in ethylene carbonate and dimethyl carbonate (1:1 by volume) was used. To make flexible batteries, pouch cells were used. In brief, the free standing electrodes were placed on a piece of aluminum foil for testing purpose (connected to the lug) however we note that freestanding electrodes do not require a substrate for mechanical support. After wetting with electrolyte, the electrode adheres to the metal foil, and after evacuating and sealing the cell, the components are compressed due to the pressure difference. The galvanostatic cycling experiments were performed with a programmable Maccor 4000 series galvanostat. The cells were discharged to 1 V and charged to 2.5 V vs. Li^+/Li^0 at various C-rates (1C = 175 mA g^{-1}).

3. Results and discussion

Phase inversion is the general term for a process of controlled polymer transformation from the dissolved liquid to solid precipitate phase. The method is a well-established large-scale process to synthesize polymer membranes for diverse applications [24]. Conversely, with regards to battery electrodes the technique is seldom applied and publications on this topic are scarce [23,25–28]. Phase inversion is often achieved by immersion precipitation, also referred to as non-solvent induced phase separation. Here a polymer containing solution is casted on a suitable support and subsequently immersed in a coagulation bath containing a non-solvent for the polymer that mixes well with the polymer solvent. The exchange of the polymer solution and the non-solvent leads to a thermodynamically unstable system, causing liquid–liquid de-mixing. This typically results in a two-phase system, *i.e.*, a solid polymer-rich phase which solidifies through processes such as gelation, vitrification, or crystallization, resulting in the membrane structure, in which a liquid polymer-poor phase induces the formation of pores in the membrane. The kinetic aspects that play a role in immersion precipitation are mostly related to the exchange rate of solvent out of, and non-solvent into, the casting solution, which in turn is related to (non-)solvent molecule size, miscibility, and the viscosity of the coating. All these factors that affect the rate of polymer solidification ultimately determine the physical morphology of membranes formed by this method [24,29].

We adopt this immersion precipitation in the conventional Li-ion electrode fabrication to achieve thick and flexible electrodes by introducing only a minor alteration of the conventional slurry casting method, in order to meet manufacturability compliance. Basically, the battery electrodes are made following the conventional slurry casting method, however, before the drying step the casted electrode is shortly submerged in a coagulation bath containing a non-solvent for the binder (Fig. 1c). This modification has surprising impact on the morphology and structural integrity of the obtained electrode. Electrodes produced by this method are over ~100 μm thick while being highly flexible, with no sign of cracking or delamination, an example is shown in Fig. 2a. Casting exactly the same slurry (as used in immersion method) but using a drying step to invert the phase of the binder, as is done traditionally, leads to a cracked and delaminated layer (Fig. 2b). This points to the beneficial effects of the coagulation step on the electrode's mechanical characteristics. This is better reflected by the fact that, after an extended period in the coagulation bath, the electrodes release themselves from the (sufficiently smooth) substrate as a self-supporting polymer bound film (Fig. 2c and d).

Remarkable levels of mass loading (similar to commercial levels) can be achieved as the self-supporting electrodes can be casted to thicknesses of hundreds of microns. Alternatively, the electrodes can be processed relatively thin and conveniently stacked on top of each other to obtain the desired mass loading. Fig. 2e shows a cross-section of a typical self-supporting electrode with a binder content as low as 5 wt% (this wt.% is close to industry standard) and these electrodes were used for the electrochemical measurements (inset of Fig. 2e). It can be observed that the electrode is characterized by a high porosity, while providing excellent interconnectivity between the individual electrode constituents, allowing the electrode to be substrate free.

To quantify the apparent difference in physical properties of both types of electrodes, tensile testing was performed. Fig. S1 shows the stress-strain curve of an immersion precipitation LTO electrode with 5 wt% PVDF and a thickness of 150 μm. The tensile strength amounts to 0.25 MPa at breaking point. This is quite remarkable since pure (100%)

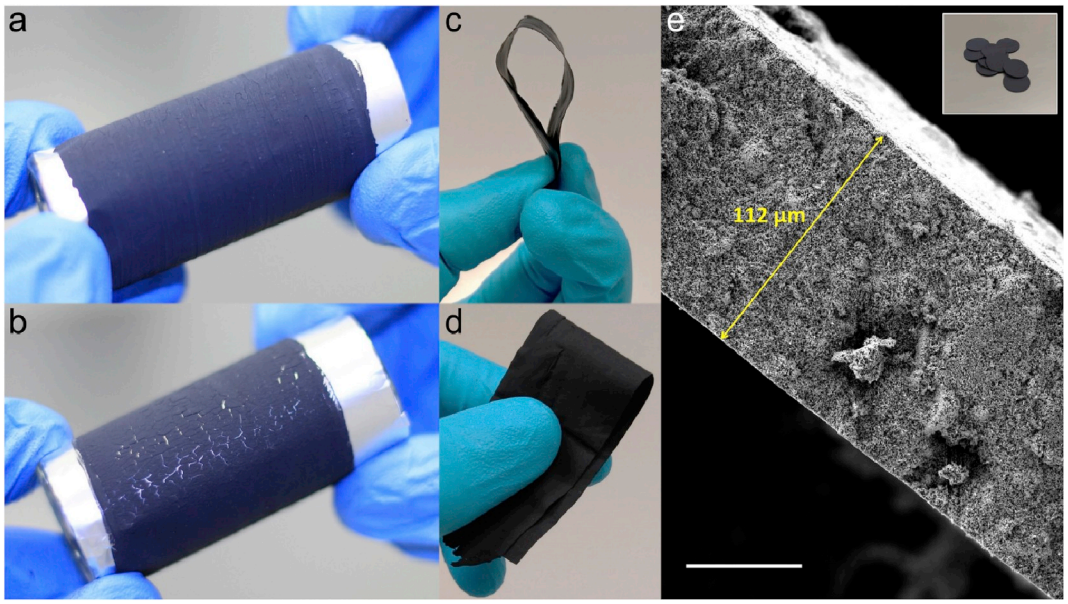

Fig. 2. Flexible ~100 µm thick LTO electrodes made by the immersion precipitation method. a) An electrode with 8 wt% binder on standard aluminum foil at a bending radius of 10 mm. Processing the same slurry by the conventional way of evaporating the solvent results in an extremely cracked and delaminated layer (b). c and d) A self-supporting, highly flexible electrode with 15 wt% binder. e) A SEM image of the cross-section of a self-supporting electrode with a binder content of 5 wt %, the scale bar represents 50 µm. These self-supporting electrodes were cut into 0.5 cm^2 disks (inset) and used in test cells.

PVDF membranes fabricated through phase inversion processes are known to have a tensile strength of 2–5 MPa [30,31]. On the contrary, when same slurry was used to make equally thick electrodes through the conventional drying technique, this yielded a cracked layer similar to the one depicted in Fig. 2b. This has presented considerable difficulties in comparing the electrodes processed via the conventional method with same thickness and mass loading, as it produced poor quality thick electrodes that are not able to withstand in the mechanical testing. The recovered cracked and brittle flakes also have extremely poor mechanical integrity and therefore could not be tested with that range of electrode thickness.

To reveal the origins of the enhanced mechanical integrity, a simple membrane, purely for imaging purposes, was made with both immersion and conventional methods, consisting of 95 wt% glassy carbon and 5 wt % PVDF. The reasons why we chose glassy carbon to reveal how PDVF is distributed across these electrodes are as follows. Firstly, they have spherical particles, and are relatively monodisperse, which allows for optimal discernibility of the binder phase. Secondly, it is extremely difficult to distinguish the PVDF network in the presence of LTO particles and Super P (Fig. 2e), which fill-up entire void space, making the visualization of PVDF almost impossible by scanning electron microscopy. Therefore, the glassy carbon and PVDF is the simplest but yet the most effective choice for demonstrating this. Fig. 3 shows the cross sections and top views of both types of electrodes. Clearly, it can be

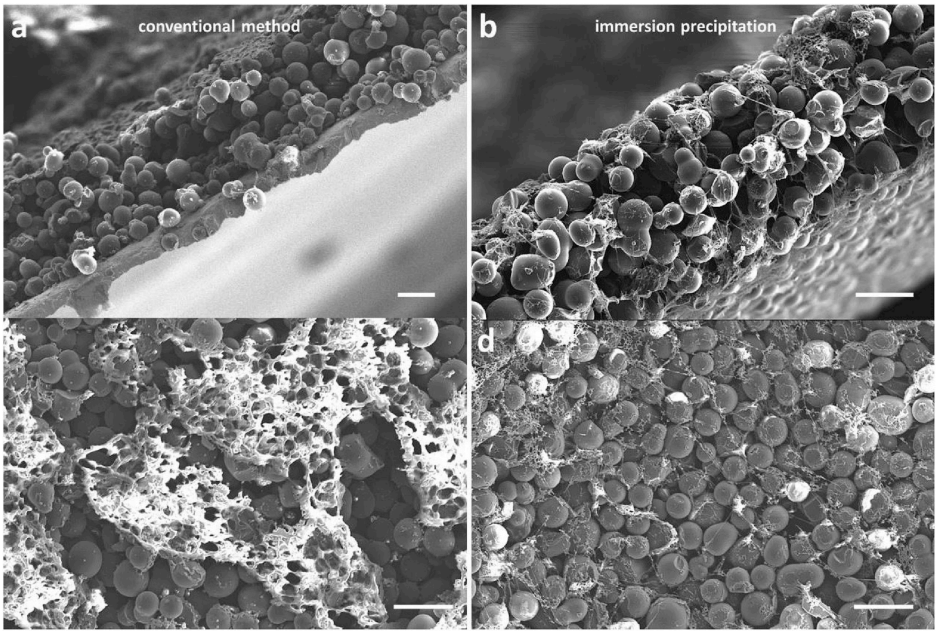

Fig. 3. Scanning electron microscopy images of 95 wt% glassy carbon membranes (5 wt% PVDF). Side-view (a) and top-view (c) of a conventionally prepared membrane on Al-foil. Side-view (b) and top-view (d) of a self-supporting membrane via immersion precipitation. The scale bars represent 20 µm.

observed that long-range cobweb like PVDF structures run throughout the immersion precipitated membrane (Fig. 3b), whereas in conventionally prepared films on Al substrates (Fig. 3a), no macroscopic PVDF networks or filaments were present. It is a general consensus that the dissolved polymer binder tends to adsorb onto battery materials (active particles and carbon) already in the slurry, i.e. before drying [32]. This process should thus occur for both methods. This binder layer on the electrode particles is able to glue neighboring particles together, i.e. forming connections on a small length scale, and seems to be the only mechanism occurring for the conventionally prepared membrane. The absence of binder or its scarce distribution across the conventionally prepared film can be further clarified by taking a look at the top of the electrode, where large aggregates of PVDF binder undergoing phase segregation/isolation can be observed. Energy dispersive X-ray spectroscopy mapping of fluorine was used to confirm the large PVDF particles (Fig. S2). This upward binder diffusion during drying is often observed in the conventional method (be it to a lesser extent than in our glassy carbon membrane used here for imaging clarity) [33,34]. The quick inversion of the binder via the immersion precipitation technique can overcome this problem by severely limiting the time for the binder to diffuse, and thus produces a homogeneous distribution of polymeric filaments throughout electrodes. Due to the ineffective precipitation of the non-adsorbed binder that occurs during drying, the ability of battery particles to glue each other at larger length scales is severely diminished, explaining the brittle nature of conventional electrodes. Conversely, during the immersion method the surplus of polymer in solution tends to precipitate as cobweb like structures, well distributed throughout the film, which, in addition to the adsorbed binder layer on the battery particles, results in a flexible layer with excellent interparticle connection. We remark that only a small fraction of PVDF is adsorbed on the particles and therefore much of it still in solution during drying, perhaps more than in a typical slurry containing also a carbon additive. It is probably caused by the limited affinity between glassy carbon and PVDF, or simply due to the small surface area of the smooth and relatively large particles. Nevertheless these experiments unambiguously establish that the distribution and secondary morphology of PVDF binder within electrodes for the two methods determine their mechanical integrity and resilience. Especially, even for materials with limited binder adsorption, immersion precipitation, as opposed to the conventional method, is able to produce flexible membranes with a homogeneous binder distribution.

As a next step we fabricated both half and full cells with the thick and flexible LTO electrodes to assess their electrochemical performance. First, as control experiments, LTO electrodes with an active mass loading of 1.5 mg cm^{-2} (0.26 mAh cm^{-2}) were tested, which is a typical mass-loading adopted in lab-scale research purposes. Fig. S3 in the supporting information shows the rate capability and cycle life tests. The electrodes are able to retain 25% of their initial capacity at a very high rate of 100C and their capacity loss is only 3% over 1000 cycles at a 5C charge and discharge rate, delivering around 140 mAh g^{-1}. The overall electrochemical performance of these electrodes is comparable to literature reports that exploit more sophisticated techniques and materials [35–38], however, as discussed earlier, such low mass loadings have little-to-no relevance with respect to commercial applications.

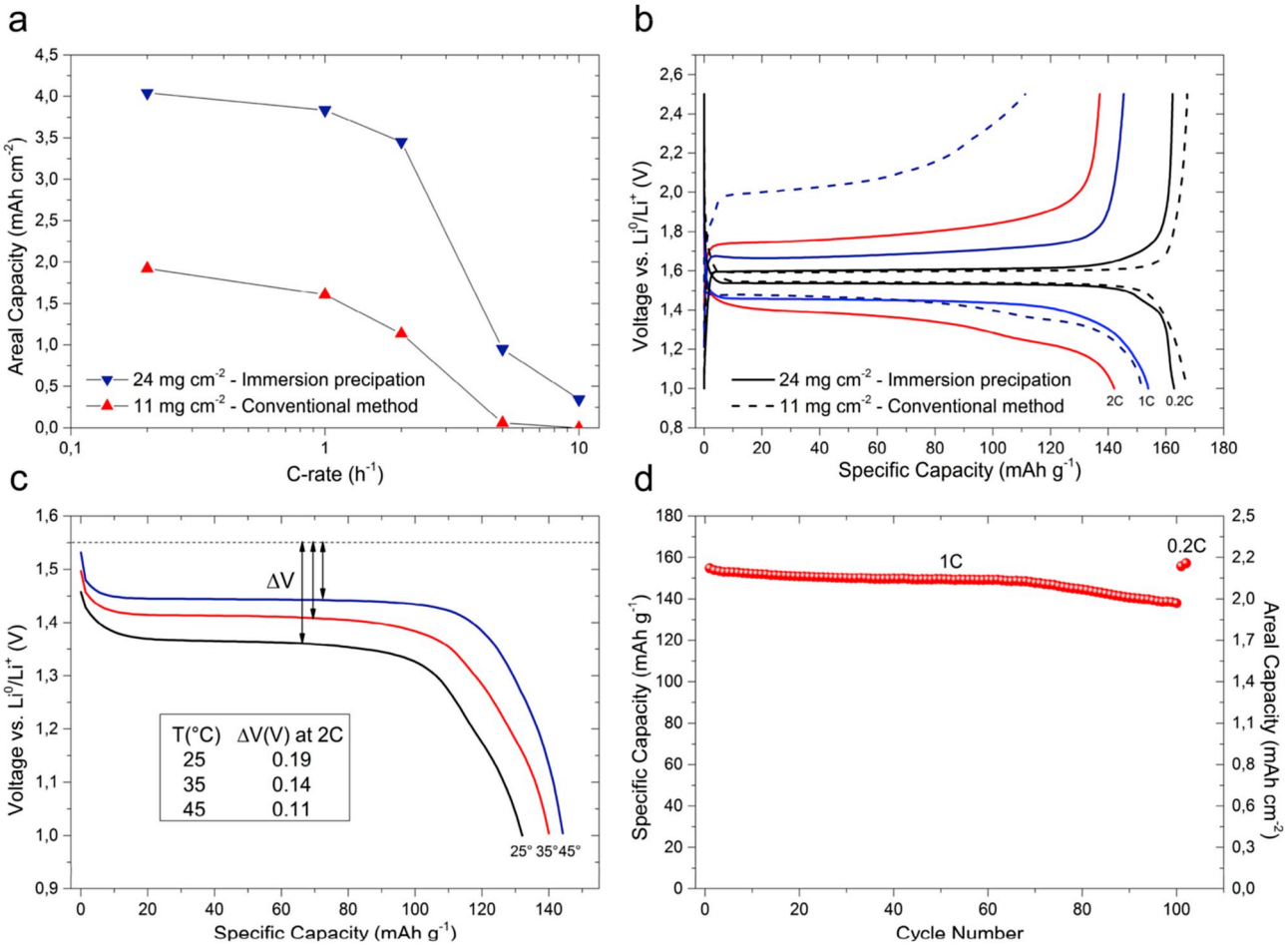

Fig. 4. Electrochemical testing of high mass-loading LTO electrodes. a) Apparent areal capacity as a function of C-rate. b) Voltage curves as a function of specific capacity for various C-rates. c) Voltage curves as a function of specific capacity of a 24 mg cm^{-2} electrode cycled at 2C, with the difference in equilibrium and discharge voltage indicated at half state-of-charge. d) Cycle performance at a rate of 1C of an electrode with a mass-loading of 14 mg cm^{-2}.

Commercial battery electrodes typically have capacities around 2 mAh cm^{-2} or higher, and an active material loading of at least 90 wt%.

To demonstrate the potential of immersion precipitation for commercial application, self-supporting electrodes consisting of 90 wt% active material, 5 wt% conductive carbon, and 5 wt% binder were prepared with a LTO mass-loading of 24 mg cm^{-2} (4.2 mAh cm^{-2}). Fig. 4a shows the rate capability of such a high mass loading electrode. At rates that are critical for practical application (0.5–2C required for electric vehicles and power tools), it shows excellent performance. In this range the electrode delivers a high capacity in excess of 3.5 mAh cm^{-2}. It is important to assess whether this capacity is attained in an energy efficient way, and therefore the voltage curves as a function of specific capacity are shown in Fig. 4b. At 2C the LTO electrode still delivers 140 mAh g^{-1}, about 80% of its theoretical specific capacity (175 mAh g^{-1}). In terms of over-potentials, the difference between the output and equilibrium voltage of the cell, it is important to consider that the associated ohmic heating would cause the battery temperature to increase. However, at increased temperature the ionic conduction improves, which in turn lowers the over-potential and thus the losses. To test the degree to which this effect takes place on electrodes prepared via immersion precipitation, temperature dependent cycling measurements were carried out, which are shown in Fig. 4c. With LTO being an anode (low-voltage) material it is important to focus on the discharge (lithiation) of the electrode, as this would correspond to the charging process in a full cell, which is required to proceed quickly. The discharge was conducted at 2C (corresponding to a full charge in 30 min). When the battery temperature was increased from 25 to 45 °C, the over-potentials decreased more than 40%, which indicates reduced efficiency losses. Assuming an operating temperature of max 45 °C, a charge rate of 2C–80% of an 80 kWh battery and an over-potential of 0.11V at a cell potential of 3.5V, one would need to cool away an amount of heat losses of 4 kWh (see Supporting Information). Such cooling amount appears practically feasible.

To compare electrodes via immersion precipitation with standard electrodes, the same slurry (as in the immersion method) was used to prepare electrodes as in the conventional way (drying method). First of all, the electrodes had to be casted relatively thin in order to obtain an acceptable level of structural integrity that allows for the fabrication of electrodes and testing. In principle it is possible to cast slurries to obtain same electrode thickness as that of immersion method but electrodes showed increased tendency to delaminate and crumble away. Solvent evaporation in the conventional method causes a larger proportion of binder to leave the active particles behind and to precipitate at the top of electrodes, which further aggravates the problem of binder deficiency across the bulk electrodes, leading to coatings with poor mechanical properties as previously hinted from mechanical testing. The dried electrodes had a thickness of 80 μm before calendaring and an areal mass loading of 11 mg cm^{-2}. Strikingly, having only less than half of the areal mass loading (compared to 24 mg cm^{-2}), these electrodes show similar or even more dependency on the (dis)charge rate (Fig. 4a) and greater over-potentials than the high-mass loading electrode prepared via immersion precipitation. During the first cycle of testing (performed at 0.5C) the voltage curves look very similar (Fig. 4b) and the Coulombic efficiencies are 99,70% and 99,74% for the immersion and conventional electrode, respectively. However, at higher rates, the over-potentials during charging for the conventional electrode were much larger than those of the much heavier immersion electrode. Already at 1C the electrode cannot be fully charged (blue dashed line Fig. 4b). At the high cycle rates (5–10C) an abrupt drop in performance is observed for both electrodes. At such high current densities the Li-ion transport through the electrolyte becomes a severe limiting factor [10,11,39]. However the mere fact that the immersion precipitation electrodes can still be cycled at these rates is significant. For comparison, recently Elango et al. [15] have proposed an interesting route to achieve electrode thickness as high as 1000 μm by combining spark plasma sintering and salt templating. As expected, rate performance tests showed that while the capacity of LFP based electrodes dropped close to zero at 2C, LTO based electrodes reached almost zero capacity at 1C, attributed to poor charge transport across electrodes. Despite the high energy density these thick electrodes can pack, they are not suitable for high-power applications for example electric vehicles.

To test the cycle stability, a high mass-loading electrode of 14 mg cm^{-2} was cycled at 1C (Fig. 4d). The electrode exhibits a very stable capacity for 70 cycles, after which it shows only a slight decline. After 100 cycles the electrode still has a specific capacity of almost 140 mAh g^{-1} which is 90% of the initial capacity. After 100 cycles at 1C, the C-rate was lowered to 0.2C. At the lower cycle rate the initial capacity is restored, indicating the fractional capacity decrease is originated from kinetics and not from the degradation of LTO electrode processed via immersion method. The capacity fade over cycling is for the largest part related to the degradation of the Li anode of the half-cell, as the development of solid electrolyte interface and dendrites with every cycle is very large due to the high areal capacity of the tested electrode [19]. In the Supporting Information (Fig. S4) we show for a cell with similar mass loading that by replacing the Li anode most of the 'lost' reversible capacity can be recovered.

It is important to note that the conventionally prepared electrodes had to be compacted (equivalent to calendaring) in order to improve their performance, whereas the electrodes via immersion precipitation can be used as prepared. Even though in this work the calendaring procedure for conventional electrodes was not optimized and therefore maximum performance most likely was not yet achieved, it still provides sufficient insights into how critical this calendaring step is for conventional electrodes, whereas for immersion precipitation electrodes it is a non-factor. This is especially surprising as electrodes obtained through the immersion precipitation process are typically characterized by a relatively high porosity [25]. Such a degree of porosity (>40%) in conventional battery electrodes often means poor inter-particle connectivity and consequently has a negative effect on their electronic conductivity and thus their performance [40,41]. Increasing the porosity can be a strategy to improve the performance of an electrode as it would result in a larger electrode/electrolyte interface for charge transfer and a better ability to accommodate volume changes of the active material during cycling [42]. This strategy can thus be pursued with the immersion precipitation electrodes, as high porosity can be achieved without compromising the inter-connectivity of the electrode particles. However, from practical application standpoint an optimal volumetric capacity is desired. This means the electrode porosity should be minimized to the point where the performance of the electrode still meets the requirement of the application. Remarkably, a compressed phase inversion LTO electrode with a porosity of only 32% and a mass loading of approximately 20 mg cm^{-2} showed only a moderate decrease in rate capability compared to its 67% porous counterpart (Fig. S5, Supporting Information).

The excellent performance of the immersion precipitated electrodes might be partly explained by the enhanced particle interconnectivity, which facilitates good electronic conductivity everywhere throughout the film. Indeed, the DC electrical resistance of immersion electrodes is 37% lower than a conventional electrode with the same mass loading (Table S1). However at the high current densities applied in this study, the ionic transport through the porous electrode would still be a limiting factor [10,11]. This is supported by the large decrease in polarization at higher temperatures (Fig. 4c) due to the decrease of the ionic resistivity of the electrolyte, whereas the electronic resistance is less temperature dependent. Therefore the enhanced performance should (for the larger part) be a result of an increased ionic transport in the electrode, which in turn is associated with the pore morphology. Ionic effects such as charge transfer resistance and ion diffusivity are reflected in the impedance of the electrode at lower and midrange frequencies [43]. Electrochemical impedance spectroscopy confirms an overall lower impedance in this range for the electrodes made via immersion precipitation (Fig. S6), which proves that immersion electrodes offer better ionic conductivity.

Also, the low DC resistance and impedance of electrodes prepared via immersion is indicative of a uniform PVDF distribution across electrodes, which provides a better interconnectivity of electrode materials. Therefore the immersion method provides a novel solution to prevent uneven binder distribution, that can lead to high electrode impedance. While the SEM images (Fig. 1) offered the first glimpse of porosity and interconnectivity in immersion electrodes, more light can be shed on the porous networks formed within both types of electrodes (immersion and conventional) by conducting mercury intrusion porosimetry. Fig. S7 shows the intrusion and extrusion of mercury as a function of pore diameter (applied pressure). Based on the volume of mercury that could infiltrate the films, their porosity is deduced to be ~60%, which is consistent with their apparent porosity based on their geometry and density. Both electrodes have very similar pore size distribution, ranging between 100 and 300 nm, characterized by a steep increase in mercury intrusion. However upon extrusion the conventional electrode shows large hysteresis. This is associated with a non-uniform pore shape and/or a poorer interconnectivity of the pores [44]. This is also reflected in the pore tortuosity and permeability measured by this method. The electrode via immersion precipitation shows a ~20% lower tortuosity (2.05 vs. 2.53) and its permeability is 2.5 times higher than the conventional electrode (91625 vs. 35307 mdarcy), which explains its enhanced ionic transport. The origin may lie in the fact that during phase inversion the non-solvent diffuses all the way through the film, from the top to the bottom, which leaves long and connected pores stretching across the whole film, whereas for conventional electrodes their pore structure is based upon much more random processes that occur during the (slow) removal of the solvent as a vapor.

We have used higher % binder (>10 wt %) only to demonstrate that our method allows for a wide concentration range of binder, which can produce ultra-flexible self-supporting electrodes. This cannot be achieved via the conventional method. Actually in lab-scale battery studies ~10% binder content in electrodes is very common, which is almost double that of commercial electrodes, but then the actual applied mass loading is typically 1–2 mg cm^{-2}, which is at least 10 times smaller than that of commercial electrodes. For this, we also show that lower binder (5%), which is close to industrial standard, can be administered in thick electrodes via immersion method for standard battery materials. Therefore, in our studies, we have achieved a well-balanced recipe using the immersion method for producing high-performance thick electrodes (with low binder) for standard batteries and ultra-flexible thick electrodes that can have either commercial level binder or more for special proposes. This of course involves a trade-off between energy density and electrode mechanical flexibility.

We further emphasis that the immersion precipitation method for battery electrodes is by no means limited to LTO [25]. Electrochemical tests of LFP and LCO electrodes and LTO-LFP full cells are supplied in the Supporting Information, Fig. S8 and Fig. S9, respectively. To indicate the scope of our method with regards to electrode flexibility we fabricated a flexible LTO-LFP pouch-cell (1 mAh cm^{-2}), shown in Fig. 5. The flexible battery is able to power a red light emitting diode (LED) even when it is completely folded (bending angle ~180°), and during battery bent (to full folding) and flat stages the LED showed no change in intensity. In terms of solvent-binder combinations, NMP and PVDF were used in this study, as it is the most widely applied solvent-binder combination for Li-ion electrodes. However, the commonly used polymers besides PVDF such as carboxymethyl cellulose and styrene-butadiene rubber have convenient non-solvents available that are miscible with their standard solvents, which suggests that they are applicable for immersion precipitation. In particular, because the widely used NMP is carcinogenic we tested the compatibility of this immersion process with DMSO that is a relatively green solvent instead of NMP. Fig. S10 in the Supporting Information compares the rate performance of electrodes processed using these two solvents. The electrodes showed almost identical performance, which indicates that DMSO can be used as effectively as NMP with the method presented in this paper. Being able to replace more toxic NMP by DMSO for electrode fabrication would be a great improvement in terms of safety and environmental impact.

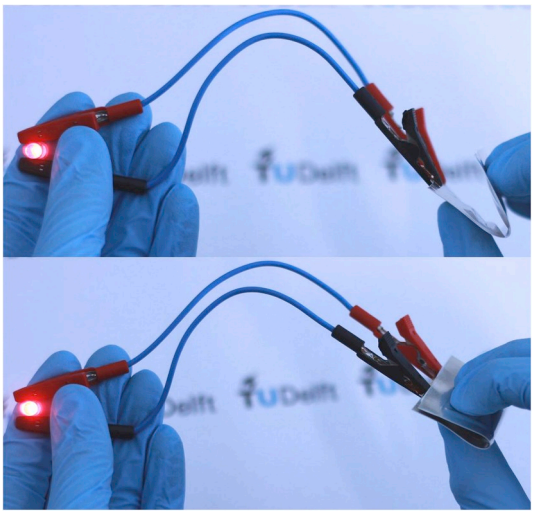

Fig. 5. A flexible LTO-LFP cell powering a red LED while being bent at different angles; 135° (top), and 180° (bottom). (For interpretation of the references to colour in this figure legend, the reader is referred to the Web version of this article.)

4. Conclusion

In conclusion, we presented a simple, potentially low-cost method based on immersion precipitation to fabricate both thick (over 100 μm) and flexible (self-supporting) electrodes without compromising the energy/power density. Owing to the unique porous structures with low tortuosity and high permeability and excellent interconnectivity of active particles facilitated by this immersion method, the thick electrodes still offer excellent electrochemical performance, in particular at rates (0.5–2C) that are required for enabling high power applications. For example, thick electrodes with only 5 wt% binder, containing commercial LTO were tested with a high mass-loading of 24 mg cm^{-2}, achieving a capacity of ~4 mAh cm^{-2} at 1C and operate at rates up to 10C. Furthermore flexible full cells (with LTO and LFP) were shown to be fully operational while they were folded at a bending angle ~180°. This method can be extended to many combinations of binders, electrode materials and (non-)solvents for achieving both ultra-thick and flexible electrodes. Our findings point to a new way for developing high performance standard batteries with thick electrodes, and thus improved energy density, as well as highly flexible electrodes without needing special additives.

Acknowledgements

We acknowledge financial support for this research from ADEM, A green Deal in Energy Materials of the Ministry of Economic Affairs of The Netherlands (www.adem-innovationlab.nl). We kindly thank F.G.B. Ooms for his help with the flexible pouch-cells, N.V. Thang for his photographs of the electrodes and test cells, and Prof. K.M.B. Jansen for his help with the tensile strength measurements. C.G. acknowledges funding received from Marie Skłodowska-Curie action H2020-MSCA-IF under grant agreement no.704659, FlexBatteries.

Appendix A. Supplementary data

Supplementary data to this article can be found online at https://doi.org/10.1016/j.jpowsour.2019.227200.

References

[1] F.M. Mulder, J. Renew. Sustain. Energy 6 (2014), 033105.
[2] G. Patry, A. Romagny, S. Martinet, D. Froelich, Energy Sci. Eng. 3 (2015) 71–82.
[3] D.L. Wood III, J. Li, C. Daniel, J. Power Sources 275 (2015) 234–242.
[4] A. Kraytsberg, Y. Ein-Eli, Adv. Energy Mater. 6 (2016) 1600655.
[5] A. Vlad, N. Singh, C. Galande, P.M. Ajayan, Adv. Energy Mater. 5 (2015) 1402115.
[6] M. Singh, J. Kaiser, H. Hahn, J. Electrochem. Soc. 162 (2015) A1196–A1201.
[7] W. Liu, M.S. Song, B. Kong, Y. Cui, Adv. Mater. 29 (2017) 1603436.
[8] S. Ahmad, D. Copic, C. George, M. De Volder, Adv. Mater. 28 (2016) 6705–6710.
[9] C.J. Bae, C.K. Erdonmez, J.W. Halloran, Y.M. Chiang, Adv. Mater. 25 (2013) 1254–1258.
[10] K.G. Gallagher, S.E. Trask, C. Bauer, T. Woehrle, S.F. Lux, M. Tschech, P. Lamp, B. J. Polzin, S. Ha, B. Long, Q. Wu, W. Lu, D.W. Dees, A.N. Jansen, J. Electrochem. Soc. 163 (2016) A138–A149.
[11] Z. Du, D.L. Wood, C. Daniel, S. Kalnaus, J. Li, J. Appl. Electrochem. 47 (2017) 405–415.
[12] J.S. Sander, R.M. Erb, L. Li, A. Gurijala, Y.M. Chiang, Nat. Energy 1 (2016) 16099.
[13] D.P. Singh, F.M. Mulder, A.M. Abdelkader, M. Wagemaker, Adv Energy Mater 3 (2013) 572–578.
[14] D.P. Singh, F.M. Mulder, M. Wagemaker, Electrochem. Commun. 35 (2013) 124–127.
[15] R. Elango, A. Demortière, V. De Andrade, M. Morcrette, V.C. Seznec, Adv. Energy Mater. (2018) 1703031.
[16] T.S. Wei, B.Y. Ahn, J. Grotto, J.A. Lewis, Adv. Mater. 30 (2018) 1703027.
[17] M.E. Sotomayor, C. de la Torre-Gamarra, W. Bucheli, J.M. Amarilla, A. Varez, B. Levenfeld, J.Y. Sanchez, J. Mater. Chem. 6 (2018) 5952–5961.
[18] Y. Gogotsi, P. Simon, Science 334 (2011) 917–918.
[19] N. Nitta, G. Yushin, Part. Part. Syst. Charact. 31 (2014) 317–336.
[20] S.J. Dillon, K. Sun, Curr. Opin. Solid State Mater. Sci. 16 (2012) 153–162.
[21] A.J. Katz, A.H. Thompson, Phys. Rev. B 34 (1986) 8179–8181.
[22] A.J. Katz, A.H. Thompson, J. Geophys. Res. B Solid Earth Planets 92 (1987) 599–607.
[23] P.P.R.M.L. Harks, C.B. Robledo, T.W. Verhallen, P.H.L. Notten, F.M. Mulder, Adv. Energy Mater. 7 (2017) 1601635.
[24] G.R. Guillen, Y. Pan, M. Li, E.M.V. Hoek, Ind. Eng. Chem. Res. 50 (2011) 3798–3817.
[25] X. Yang, Y. Chen, M. Wang, H. Zhang, X. Li, H. Zhang, Adv. Funct. Mater. 26 (2016) 8427–8434.
[26] S.S. Zhang, D.T. Tran, J. Power Sources 211 (2012) 169–172.
[27] I. Byrd, H. Chen, T. Webber, J.L. Li, J. Wu, RSC Adv. 5 (2015) 92878–92884.
[28] I. Byrd, J. Wu, Electrochim. Acta 213 (2016) 46–54.
[29] A.K. Holda, I.F.J. Vankelecom, J. Appl. Polym. Sci. 132 (2015) 42130.
[30] W.B. Zhang, Z. Shi, F. Zhang, X. Liu, J. Jin, L. Jiang, Adv. Mater. 25 (2013) 2071–2076.
[31] J.T. Jung, J.F. Kim, H.H. Wang, E. di Nicolo, E. Drioli, Y.M. Lee, J. Membr. Sci. 514 (2016) 250–263.
[32] V. Wenzel, H. Nirschl, D. Notzel, Energy Technol. 3 (2015) 692–698.
[33] F.Y. Su, L.Q. Dai, X.Q. Guo, L.J. Xie, G.H. Sun, C.M. Chen, J. Energy Storage 14 (2017) 82–93.
[34] B.G. Westphal, A. Kwade, J. Energy Storage 18 (2018) 509–517.
[35] J. Coelho, A. Pokle, S.H. Park, N. McEvoy, N.C. Berner, G.S. Duesberg, V. Nicolosi, Sci. Rep. 7 (2017) 7614.
[36] Z. Yao, X. Xia, C.-a. Zhou, Y. Zhong, Y. Wang, S. Deng, W. Wang, X. Wang, J.C. Tu, Adv. Sci. (2018) 1700786.
[37] X. Jia, Y. Lu, F. Wei, Nano Res 9 (2016) 230–239.
[38] J. Xie, P. Harks, D.J. Li, L.H.J. Raijmakers, P.H.L. Notten, Solid State Ion. 287 (2016) 83–88.
[39] H.H. Zheng, J. Li, X.Y. Song, G. Liu, V.S. Battaglia, Electrochim. Acta 71 (2012) 258–265.
[40] C. Fongy, A.C. Gaillot, S. Jouanneau, D. Guyomard, B. Lestriez, J. Electrochem. Soc. 157 (2010) A885–A891.
[41] Y. Orikasa, Y. Gogyo, H. Yamashige, M. Katayama, K.Z. Chen, T. Mori, K. Yamamoto, T. Masese, Y. Inada, T. Ohta, Z. Siroma, S. Kato, H. Kinoshita, H. Arai, Z. Ogumi, Y. Uchimoto, Sci. Rep. 6 (2016) 26382.
[42] A. Vu, Y.Q. Qian, A. Stein, Adv. Energy Mater. 2 (2012) 1056–1085.
[43] X.C. Sun, M. Hegde, Y.F. Zhang, M. He, L. Gu, Y.Q. Wang, J. Shu, P. V. Radovanovic, B. Cui, Int. J. Electrochem. Sci. 9 (2014) 1583–1596.
[44] H. Giesche, Part. Part. Syst. Charact. 23 (2006) 9–19.